IEEE Access
Multidisciplinary | Rapid Review | Open Access Journal

Received August 2, 2019, accepted September 8, 2019, date of publication September 18, 2019,
date of current version September 30, 2019.

Digital Object Identifier 10.1109/ACCESS.2019.2942184

Cuffless and Continuous Blood Pressure Monitoring Using a Single Chest-Worn Device

JONGHYUN PARK[1], SEUNGMAN YANG[1], JANGJAY SOHN[1], JOONNYONG LEE[1], SARAM LEE[2], YUNSEO KU[3], (Member, IEEE), AND HEE CHAN KIM[2,4], (Member, IEEE)

[1]Interdisciplinary Program for Bioengineering, Graduate School, Seoul National University, Seoul 08826, South Korea
[2]Institute of Medical and Biological Engineering, Medical Research Center, Seoul National University, Seoul 08826, South Korea
[3]Department of Biomedical Engineering, College of Medicine, Chungnam National University, Daejeon 34134, South Korea
[4]Department of Biomedical Engineering, College of Medicine, Seoul National University, Seoul 08826, South Korea

Corresponding author: Hee Chan Kim (hckim@snu.ac.kr)

This work was supported by the Bio and Medical Technology Development Program of the National Research Foundation (NRF) funded by the Korean Government (MSIT) under Grant 2016M3A9F1939646.

ABSTRACT Continuous blood pressure (BP) monitoring in daily life is needed to enable early detection of hypertension and improve its control. Although pulse transit time (PTT)-based BP estimation represents a promising approach, it still lacks of performance in systolic blood pressure (SBP) estimation and its use in daily life is limited owing to the requirement of bulky systems for measurement of PTT. This study aims at developing a wearable system providing continuous PTT measurement and enhanced SBP estimation for continuous BP monitoring. A single chest-worn device was developed, which measures the photoplethysmogram and seismocardiogram simultaneously, and thereby obtains PTT by time difference between two signals. A multivariate model using the seismocardiogram amplitude (SA) in conjunction with PTT was proposed for SBP estimation, and validated against 30 healthy males (31.47 ± 7.23 years old). Performance of the proposed model was compared with that of conventional univariate models using PTT or pulse arrival time in two types of BP interventions, and for the verification of real use in daily life, performance assessment with calibration and BP monitoring in daily life were conducted. The results suggested that the proposed model (1) outperformed the conventional models, (2) showed potential to be generalized with just a simple calibration, and (3) demonstrated the potential of continuous BP monitoring in daily life. In conclusion, the presented system provides an improved performance of continuous BP monitoring by using a combination of PTT and SA with a convenient and compact single chest-worn device, and thus, it can contribute to mobile healthcare services.

INDEX TERMS Continuous blood pressure monitoring, mobile healthcare, wearable device, pulse transit time, photoplethysmogram, seismocardiogram.

I. INTRODUCTION

Hypertension is widespread in the US and is the major factor of cardiovascular disease, the leading cause of death in 2014 [1]–[4]. To prevent such critical events, hypertension should be detected by checking one's blood pressure (BP) status and properly managing it in its early stage. However, measurement of BP is generally performed in a clinical setting with a conventional inflatable cuff-type device, which provides only a single or intermittent snapshot of varying BP and could thus even be misleading in representing ''true'' BP status [4]. Thus, continuous BP monitoring (CBPM) in daily life is recommended [4], but the cuff-based BP measurement system has limited application owing to discomfort and inconvenience.

As one of the promising techniques to provide convenient measurement of BP, the pulse transit time (PTT)-based approach is receiving increasing attention. PTT is defined as the time delay for the BP wave to propagate between two arterial sites, and it is considered the surrogate marker of BP with greatest potential. Although numerous studies have attempted to employ the PTT–BP relationship for cuffless BP monitoring, most studies have used the pulse arrival time (PAT) instead, owing to its simplicity in measurement [5]–[10]. PAT is measured by employing the R-peak in an electrocardiogram (ECG) as proximal timing reference

The associate editor coordinating the review of this manuscript and approving it for publication was Rajeswari Sundararajan.

(timing when the BP pulse begins) and the early rise point of the photoplethysmogram (PPG) as distal timing reference (timing when the BP pulse arrives) and calculating the time difference between them. Although the R-peak in ECG does not represent the beginning of the BP pulse (since considerable time delay between the R-peak in ECG and ejection of blood from the left ventricle (LV) exists), it has been widely used to serve as proximal reference. It is thought that the simplicity of using the ECG outweighs the possible issue of including the time delay. However, this time delay nearly overlaps with the pre-ejection period (PEP), which is defined as the time delay between the Q-peak in ECG and the aortic valve opening time, has different mechanisms for responding to the BP change, and thus has been reported to cause a significant adverse effect in using PTT–BP relationship [11]–[13]. Therefore, efforts to eliminate the portion of PEP by using different bio-signals other than ECG have been made [14]–[17]. However, the modalities to measure PTT proposed so far are questionable in terms of practicality, and lack the potential for being utilized in daily life. Most of the previous studies mainly focused on validating the efficacy of the PTT in relatively static circumstances or in surgery, which are mostly controlled settings.

Additionally, even the PEP-excluded PTT does not provide satisfactory results of BP estimation. While PTT has shown good correlation with DBP or MBP, it has produced less satisfactory results in terms of relationship with SBP [12], [17]. [18], compared that PAT has often exhibited better correlation with SBP than PTT [17]. It was thought that PTT, as a single variable, could not track both DBP and SBP as the correlation between the two BPs decreases in certain cases and is not always high [19], [20].

Thus, there are attempts to independently estimate the difference between SBP and DBP, pulse pressure (PP), which causes uncorrelated movements of BP and degrades the performance of the PTT-based approach, by incorporating a new variable, and summate the estimated DBP and PP to derive the SBP [9], [10]. As PP depends on cardiac ejection, arterial stiffness, and timing of wave reflections [21], [22], the PTT related with arterial stiffness may be insufficient to account for changes in PP, whereas the arterial stiffness is the major determinant of DBP by vessel wall properties. Given that the rise in PP is often more attributed to the increase in cardiac ejection [22], an indicator of cardiac ejection may be utilized as potential marker of PP, and thus, complement the SBP estimation previously done with only PTT.

Recently, the seismocardiogram (SCG), precordial vibration of cardiac movement, has gained significant interest as a signal to provide rich information regarding cardiac motions [23]–[29]. Previous works have shown that a particular feature point of the SCG waveform coincides with the opening of the aortic valve according to simultaneous observation by an echocardiogram [24], [30], and features derived from SCG have been validated for estimating cardiac ejection [24], [25]. Thus, SCG could be utilized to serve proximal timing reference and also to provide an indicator of PP. However, the use of SCG is, owing to the signal source, limited in terms of measurement sites. SCG is usually measured in the vicinity of the sternum, which hinders the combination with the PPG serving distal timing reference as it is difficult to acquire a high-fidelity PPG waveform on the chest surface, which lacks of blood perfusion as compared to other locations such as the finger-tip, toe, and ear.

Therefore, the objective of this research is to propose a wearable system providing continuous measurement of PEP-excluded PTT and a SCG-driven covariate to improve the conventional PTT-based approach in order to realize cuffless and continuous BP monitoring in daily life. For this objective, we 1) developed a single chest-worn device that measures SCG and PPG simultaneously, 2) proposed a new model to complement the PTT-based BP estimation by incorporating a SCG parameter, the early peak amplitude of SCG (SA), as a potential indicator of PP, and 3) validated the efficacy of the model by comparing it with conventional PTT and PAT models, and assessed practical aspects such as the generalization ability of the model after a calibration process and its usability in daily life.

II. METHODS AND MATERIALS

A. SYSTEM DESIGN

The core design of the proposed system aims to enable the measurement of PPG and SCG on the chest with a single compact and light device. Fig. 1(a) shows the overall system block diagram, consisting of bio-signal sensors, pre-amplification analog circuits, digital circuits, a power management unit, a communication unit, and external data acquisition units. Three types of sensors were employed.

To measure PPG on the chest, three pairs of optical sensors, each consisting of one 850 nm wavelength infrared LED (SFH4059, OSRAM, Germany) and two photodiodes (VBP104S, Vishay, US) were used to enhance the SNR of the PPG. The three optical sensor pairs were placed apart from each other to widen the sensing area, as the blood perfusion beneath the skin of the chest is not abundant for PPG measurement compared to other areas, such as the finger, earlobe, and toe, which are traditionally used as PPG measurement sites. Each output current from the three optical channels was converted to voltage using a trans-impedance amplifier (TIA) circuit.

To boost the SNR of PPG, a DC offset subtraction feedback loop was employed. This loop monitored the DC level of PPG by MCU, which is directly proportional to the amount of light emitted from the LED. Depending on the current DC level, the MCU decided the corresponding output of the digital to analog converter (DAC), and thereby controlled the offset current using a feedback resistor (Fig. 1(b)), which prevents the circuit from the saturation that occurred frequently due to high intensity of light. Thus, this enabled the use of high intensity of light without concern for saturation, which results in a high SNR of the PPG.

For SCG, the anteroposterior axis output of a low-power analog accelerometer (ADXL327, Analog Devices, US) was

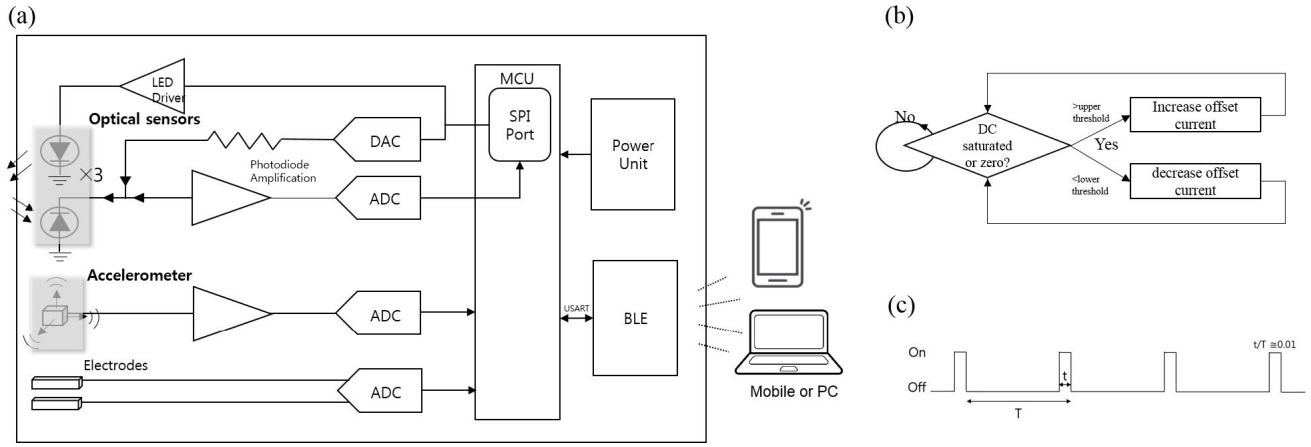

FIGURE 1. System block diagram and specialized technique applied to the system. (a) The system consists of bio-signal sensors, pre-amplification analog circuits, digital circuits, power management unit, communication unit, and external data acquisition units. Specialized technique applied to the system. (b) Feedback algorithm to maintain proper DC offset level. Depending on whether DC offset is saturated or zero, the offset current is regulated. (c) LED dimming control scheme to reduce LED power. LED turned on every a hundredth of a period (t/T∼0.01).

used. The accelerometer had a full-scale range of ±2g, and this small full-scale range may be appropriate for sensing a low level of vibration, such as that of the SCG. An internal low-pass filter with cutoff frequency of 50 Hz was used to suppress aliasing in the ADC process.

Furthermore, ECG electrodes were used for an auxiliary purpose: to assist signal processing for its robustness against noise. For simple ECG measurement, a widely used two-electrode configuration was employed with common-mode biased voltage. The electrode metals were a copper base coated with platinum to increase bio-compatibility, forming a single lead with 5 cm distance across the chest.

An analog circuit was minimally designed to prevent the phase shift of signals, which may affect the inter-waveform time measurements. Only a simple and basic analog circuit, a trans-impedance amplifier (TIA) and a first-order low pass filter, was used. However, our design employs a high resolution ADC (ADS1298, TI, US) to complement resolution problems, as the phase distortion by the analog filter is a crucial issue when calculating the time difference between signals. Most of the filtering and amplification was conducted in the software.

The hardware was designed to reduce power consumption to enable continuous monitoring in a long-term period. We used three LEDs consuming up to 180 mA (60 mA each) in total during normal operation to acquire high-fidelity PPG in the chest. However, we employed the strategy that controls the dimming frequency and timing of the LEDs. As Fig. 1c shows, during one period of ADC sampling, the LED turned on every hundredth of a period (T), which lowered the current consumption of the LED down to 1% of that in normal operation and enabled a substantial reduction in power consumption of the whole system. Additionally, using a Bluetooth low energy (BLE) module and MCU (ATMEGA168, Atmel, US), the whole system consumed less than 10 mA during monitoring, enabling more than one day of continuous monitoring with a 280 mAh small-sized lithium polymer battery (30 mm × 25 mm × 4 mm), and was designed to be recharged with a micro USB cable, as it is done in a mobile phone, for continuous monitoring in daily life.

The acquired and digitized signal data were transferred via a Bluetooth module (BoT-CLE310, Chipsen, South Korea) to an external data acquisition system, such as a mobile application and PC software platform, which were also developed for convenient and practical use of the system.

The design of the printed circuit board (PCB) and the case were considered to improve contact with the chest. All analog and digital circuits were implemented on a customized PCB comprising three rigid pieces connected by flexible bridges to flexibly conform to the curvature of the torso. The flexible PCB was encased in a curved hard-case, which is also capable of flexion depending on the curvature of the torso. The developed device measured 40 mm in length, 76 mm in width, 18 mm in thickness, and weighed 27.5 g, including the hard case. (Fig. 2).

B. REAL-TIME SIGNAL ACQUISITION AND PROCESSING

Two types of data acquisition platforms were developed. First, mainly for the purpose of validation in the in-lab condition, where a PC is easily equipped, a PC-based graphical user interface (GUI) software was developed (MATLAB 2018a; The MathWorks, MA, USA). This collects data from the developed device via a serial port and displays the raw waveforms of three signals (PPG, SCG, and ECG) and the processed signal in one heart beat period along with the reference BP, which is recorded simultaneously for validation in the BP estimation stage. The signals and reference BP are saved by pushing the designated button, and the time lapse is also shown in the front to track the recording time (Fig. 3(a)).

The second platform is the mobile application for daily monitoring. The mobile application is based on Android OS and is not supported for the iOS. It automatically pairs with

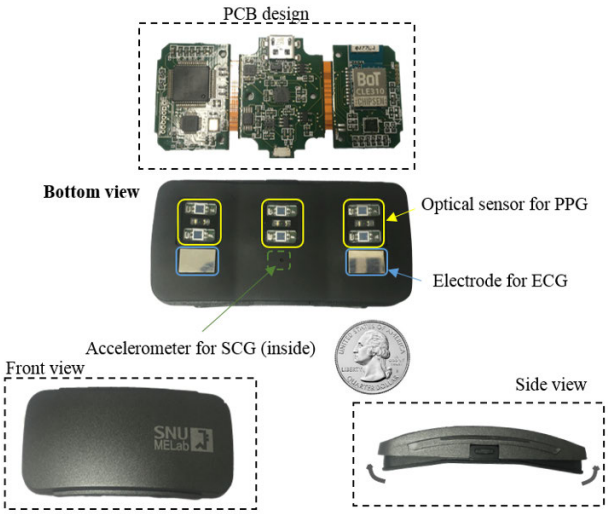

FIGURE 2. Printed circuit board and case design.

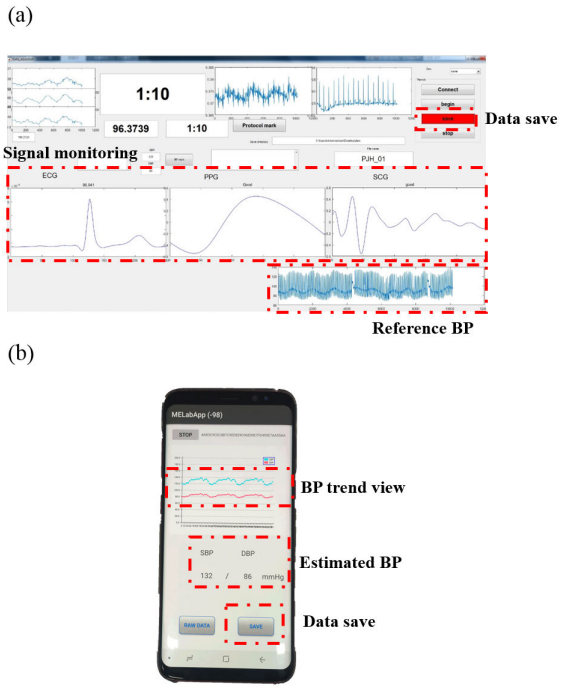

FIGURE 3. Data acquisition program. (a) A PC-based graphical user interface data acquisition program was developed, which was designed to show the processed signal in one heart beat period along with the reference BP. (b) Mobile application based on Android OS was designed to auto-connect with the developed device, save received data, and show processed signals, parameters, and estimated BP.

the developed device and collects the data in a daily life. It displays the raw signals, processed parameters such as PAT, PTT, and HR, and the final estimated BP, depending on the user's choice (Fig. 3b). By setting the period of trend view longer, users can track one's BP during a long time, and thus, evaluate BP changes in real practice.

The acquired raw signals were processed using MATLAB to remove noise from the motion artifact, baseline wandering, and respiratory signal. The SCG and ECG signal was band-pass filtered with cutoff frequencies at 0.3 Hz and 50 Hz. The raw PPG signals from three optical channels were low-pass filtered with a cutoff frequency of 10 Hz considering the frequency characteristic of PPG, and high-pass filtered with a cutoff frequency of 0.3 Hz. Digital filters without phase shift were used to prevent signal shifting during filtering.

Afterwards, we employed the ensemble averaging method to extract the averaged signal in one cardiac cycle. In 10 s of signals, the ECG R-peaks were identified for the ensemble standard. PPG and SCG signals between two consecutive R-peaks were segmented and all segments of PPG and SCG between two consecutive R-peaks were averaged, which results in one waveform for PPG and SCG in a single cardiac beat in 10 s.

Since three PPG channels were used, we obtained three PPG waveforms, one of which was selected according to the developed selection criteria. These criteria were based on the morphology of segmented PPG waveforms by cardiac beat. We designed conditions (e.g., whether clear troughs or peaks occur in the waveform within 100 ms) that a typical PPG waveform (average obtained from experiments) would meet, scored a PPG waveform by checking the number of conditions it meets, and selected the waveform that met the most conditions.

After one PPG waveform and one SCG waveform were obtained, the characteristic points were detected. In the SCG waveform, the maximum peak, named AO according to the designation of early works on SCG [25], [26], was detected, the timing of the maximum peak was calculated, and the maximum amplitude of the SCG waveform (maximum downward peak prior to the AO point - maximum peak) was regarded as the SCG amplitude (SA). In the PPG waveform, the intersecting tangent (IT) point [31] (which is the intersecting point between the tangent to the PPG max slope and the tangent to the diastolic minimum) was detected. Using the PPG IT point, PAT could be measured with sufficient time delay, given that the course of propagation to subcutaneous region of chest includes large central elastic vessels such as ascending aorta, and carotid, and small portion of peripheral artery [16]. Then, the time difference between the AO point and PPG IT was regarded as PTT (Fig. 4), which is minimally affected by vasomotion frequently occurred in the peripheral artery [11], and thus could be reliable surrogate marker of BP.

C. PRINCIPLE OF BP ESTIMATION

PTT is the time delay for the BP wave to propagate between two arterial sites. Thus, PTT is in inverse relationship with PWV. PWV is known to be closely associated with arterial elastance, which is commonly modeled by Moens–Kortewerg equation assuming an artery as an elastic tube [32]–[35] as follows:

$$PWV = \sqrt{\frac{Eh}{2\rho r}} \tag{1}$$

where E is the arterial elastance, h is thickness of the vessel wall, r is radius of the vessel, and ρ is density of blood. By this model, PTT is inversely related to arterial elastance.

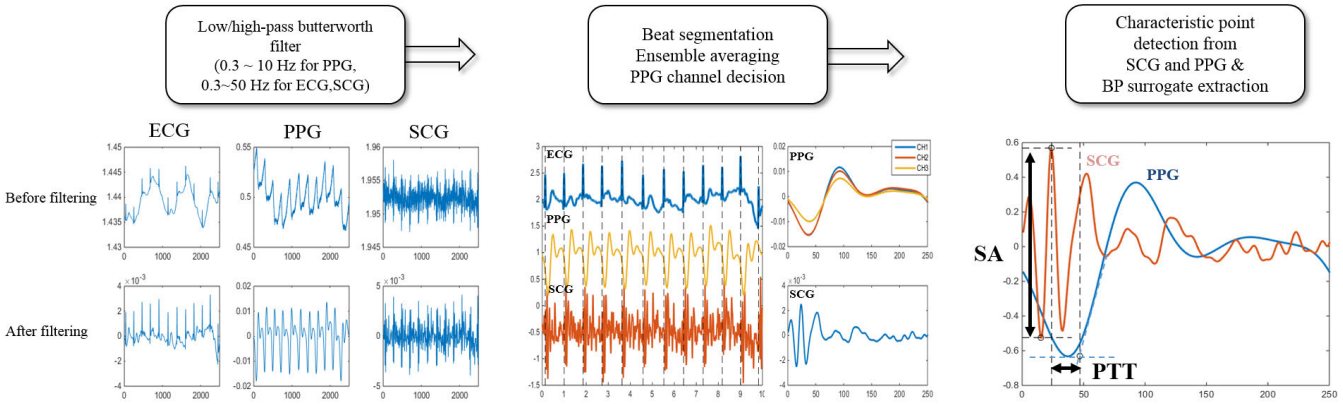

FIGURE 4. Flow chart of signal processing. First, acquired signals were low and high band pass filtered with different cutoff frequency bands depending on the signal (0.3–10 Hz for PPG, 0.3–50 Hz for ECG and SCG). Then, heart beat was segmented by R-peak detection and using ensemble averaging technique, PPG and SCG waveform from each heart beat period were averaged, resulting in one waveform of PPG and SCG. Single PPG waveform was chosen based on the developed criteria. Afterwards, in SCG waveform, maximum peak and maximum downward peak prior to AO point were detected and SCG amplitude (SA) was calculated. In PPG waveform, intersecting tangent (IT) point was detected and PTT was calculated between AO point and PPG IT point.

The arterial elastance was empirically modeled by the Hughes equation [36] as follows:

$$E = E_O e^{\alpha P} \tag{2}$$

where E is the artery elastance, E_O is the base elastance, α is a model coefficient, and P is BP. Hughes found out by experimentation that BP is logarithmically related to arterial elastance.

Consequently, combining the two equations above results in the relationship between BP and PWV or PTT, which is written as follows:

$$PWV = \sqrt{\frac{E_O e^{\alpha P} h}{\rho 2r}} \tag{3}$$

Squaring both sides and taking the log of each side yields

$$P = \frac{1}{\alpha} \ln PWV + \frac{2}{\alpha} \ln \frac{2\rho r}{E_0 h} \tag{4}$$

where the relationship between BP and PWV is explicitly expressed.

In deriving (4), BP is originated from Hughes equation [36], in which, according to his research, BP indicates the mean arterial blood pressure (MBP). Therefore, many research groups consider PTT as a marker of MBP [16], [37]–[39]. Other researchers believe that PTT should correspond best to DBP because PWV initiates in a diastole state and the level of the waveform feet is DBP [11], [13], [17]. We will follow here the latter group, and thus, estimate DBP using PTT. However, as MBP is more closely related to DBP than SBP and it is rare that DBP and MBP move in different directions, it is thought that the two approaches would not yield great differences in terms of error.

Rewriting (4) and substituting BP as DBP results in the following equation:

$$DBP = \frac{1}{\alpha} \ln PWV + \frac{2}{\alpha} \ln \frac{2\rho r}{E_0 h} \tag{5}$$

If PWV is substituted with L/PTT, where L is the certain pulse travel distance,

$$DBP = -\frac{1}{\alpha} \ln PTT + \frac{2}{\alpha} \ln \frac{2\rho r}{E_0 h} + \frac{1}{\alpha} \ln L \tag{6}$$

PP was approximated by linear modeling using SA, as the association of SA with cardiac ejection [24], [25] can be further applied to PP, assuming that the change in PP is solely caused by change in cardiac ejection.

$$PP = p_1 SA + p_2 \tag{7}$$

where p_1 and p_2 are linear coefficients relating SA with PP.

Consequently, SBP can be derived by summating DBP and PP, estimated by PTT and SA, respectively, as follows:

$$SBP = -\frac{1}{\alpha} \ln PTT + p_1 SA + \frac{2}{\alpha} \ln \frac{2\rho r}{E_0 h} + \frac{1}{\alpha} \ln L + p_2 \tag{8}$$

Further, SBP and DBP can be rewritten in a simplified form as follows:

$$SBP = a \ln PTT + bSA + c \tag{9}$$

$$DBP = a' \ln PTT + b' \tag{10}$$

where a, b, c, a', and b' are treated as subject-specific parameters. Details about determination of those parameters are described in the 'G. DATA ANALYSIS' section.

D. STUDY PROTOCOL

The study consisted of three stages with different purposes: 1) to validate the efficacy of the proposed model; 2) to assess the model when generalized to new subjects with a simple calibration process; and 3) to validate the system for continuous monitoring in daily life;

For the first stage, the subjects were asked to wear the developed device around the chest and the finger-cuff type reference BP measurement device (Finometer, Finapres Medical Systems, Netherlands), which is based on a volume-clamp method. We acquired the bio-signal data from the

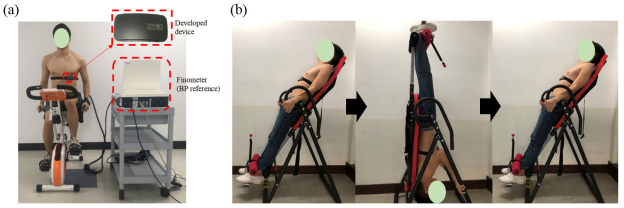

FIGURE 5. A subject in experimental setup. (a) Subject cycling with the developed device and reference BP. (b) Subject on the tilting machine. First for 3 min, the subject was in head-up position, followed by head-down tilt by −90° for 3 min and returned instantly to upright position.

device and the reference BP while inducing BP changes in two ways (Fig. 5). The two types of intervention employed were cycling and head down/up (HDU) tilt, each of which induces dominant changes in PP and DBP, respectively. The two interventions were chosen to validate the proposed model in the two contrary cases of BP changes (dominant changes in PP and DBP), considering that the model should be used in various types of BP changes in daily life.

Cycling is one of the widely used interventions to perturb BP [40]–[43], especially because it can greatly increase BP with ease. During cycling, the activated sympathetic nerve greatly increases HR and SV, and thus, cardiac output (CO), while total peripheral resistance (TPR) is decreased owing to vascular dilation in the active muscle [44], which results in a relatively small increase in DBP and great increase in SBP. Therefore, we regarded the cycling test as a PP dominant BP change protocol.

For the second type of intervention, an HDU change was performed. Orthostatic stress occurs when a subject stands up quickly, which causes the reduction of venous return due to pooling of the blood volume in the lower body by the gravitational force [45]. In the orthostatic phase, BP drops rapidly and instantly within a few seconds owing to the lack of venous return and the concomitant decrease in SV, and it rebounds to normal owing to the baroreflex mechanism, which initiates vasoconstriction and thereby greatly increases the total peripheral pressure (TPR) within 10 to 20 s in healthy subjects [45], [46]. For this rebound of BP, the increase in TPR has much greater importance than CO change [47]–[50], which results in a great increase in DBP and a relatively small change in PP, thereby increasing SBP in almost the same degree as DBP. Therefore, we regarded the BP change period when BP rebounds by the unloaded baroreceptors, initiating the increase in TPR, as the DBP-dominant BP change.

In the second stage, to assess the generalization ability of the proposed model, subjects participating in the second stage were asked to remain still while the model was calibrated for each subject, as will be described in the Data Analysis section and begin to cycle in the same way as done in the first study.

At the final stage, the developed device was attached in the same way as was done in the previous studies and, for reference BP, the subjects were asked to wear a portable ABPM (ABPM 7100; Welch-Allyn, US), which consists of a cuff designed to wrap around the upper arm, and a main head, which controls the cuff, records the data, and is designed to hang across the body (Fig. 6). They were asked to behave freely during a day without particular regulation on the type of activity. It was only asked that when the reference device measures BP, they should stay as still as possible because movements considerably affect the reliability of a reference BP value. The subjects were told that they could take off the device as they wanted, such as during a shower or exercise. The time when the study began differed depending on their preferences. The signals, estimated BP, and reference BP were recorded via the developed android-base mobile application for up to 24 h, including the sleep period. The overall protocol is depicted in Fig. 7.

FIGURE 6. Setup of daily BP monitoring. Subjects wore the developed device and reference oscillometric method-based ABPM carrying the mobile phone that collects the data, shows processed signals, and estimates BP online. They were asked to behave freely during a day, without particular regulations on any type of activity.

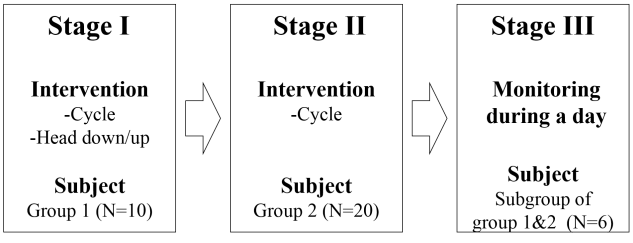

FIGURE 7. Flow diagram of the study protocol.

E. SUBJECTS

Under the Institutional Review Board approval obtained from the College of Medicine in the Seoul National University

and Hospital (IRB No. H-1701-111-826), a total of 30 male subjects (31.47 ± 7.23 years), without any previous history of cardiovascular conditions, were recruited. Informed consent was obtained from all individual participants. For the first stage of the study, where the proposed model is compared with the conventional models in two different interventions, 10 male subjects (29.70 ± 5.46 years) were first recruited. The volunteers were young and healthy, and their BP range was in a normotensive range.

For the second stage of the study, 20 subjects (32.35 ± 7.96 years), whose demography was relatively more diverse than the subject pool in the first study, were recruited afterwards. There was one subject whose entry BP range was within stage 1 hypertension level (140–160 mmHg), 8 pre-hypertensive subjects whose entry SBP were in between 120–140 and DBP in between 80–89, and normotensive subjects whose entry SBP was less than 120 and DBP less than 80. The age of the subjects was relatively more diverse than the subject pool for study 1, ranging from 25 to 54.

For the last stage, to monitor BP in daily life, nine subjects, who have already taken part in the previous stages, volunteered.

As the subjects were enrolled in different periods depending on the purpose of the study, the number of participants and demography of the subject pool was different according to the study protocol.

F. DATA COLLECTION

After placement of the device, subjects were instructed to cycle (Fig. 5(a)) for 10 min with 3 min of rest and 5 min of a recovery phase prior to and after the exercise. During cycling, the same intensity of the exercise was applied to all subjects; however, in some cases when the BP change was minimal, the intensity was increased by a change in the speed and pedaling load. Following the exercise protocol, the subjects were laid on a head-up/down tilt machine (Fig. 5(b)). At the beginning, the subjects were in head-up positions for 3 min, then the machine was tilted down to −90° to obtain a subject upside-down posture for 3 min. After the head-down position, the machines returned to the upright position instantly to induce orthostatic stress and were held for 5 min. During the protocol, PPG, SCG, and ECG from the device and reference BP were acquired continuously by the data acquisition PC program.

For data in the first stage, we extracted the BP-related parameters (PAT, PEP, PTT, and SA) for each subject record. Each BP level (SBP, DBP, and PP) was calculated in the same length of window (10 s) as performed for other parameters. In every window of 10 s, sliding by 2 s, the highest peaks and lowest troughs of BP waveform were detected and averaged, for SBP and DBP, respectively. PP was calculated by the difference between the averaged SBP and DBP. For each cycling subject in the first stage, we extracted five pairs of BP-related parameters (PAT, PEP, PTT, and SA) and BP values (SBP, DBP, and PP) in the rest and exercise phases by evenly segmenting the phases and averaging them over the segmented period, respectively, to minimize noise. This resulted in a total of 10 pairs of datasets for each subject in the cycling protocol. In the case when BP rose rapidly during the exercise, which often caused error in the BP measurement device, and SBP increased excessively, exceeding more than 35 mmHg compared to that in the rest phase, five pairs were obtained instead in the recovery phase, in the same way as in the other phases, before BP returned to baseline. For each subject in the HDU protocol, the same number of datasets (N=10) from the cycling protocol was obtained in the interval between the point when BP dropped to a minimum by HDU change and the point when BP returned to baseline. Finally, a dataset comprising 20 pairs of BPs and parameters were obtained from each subject involved in the first stage.

For the second stage, a single pair of BPs and estimation parameters (PTT, and SA) for calibration was averaged over the first half of recording in the rest phase, and three pairs of BPs and the parameters were extracted in the rest of the rest phase and exercise phase, respectively, by evenly segmenting each phase into three periods and averaging them over the segmented period.

In the final stage, the ABPM was set to automatically measure BP twice per hour during daytime and once per hour during nighttime. The estimation parameters were averaged over 6 min each time the reference BP was measured by the ABPM device (3 min prior to and after BP measurement). In 6 min, if less than half of the parameters were acquired owing to low signal quality of either PPG, SCG, or ECG, a pair of the measured BPs and parameters at that time stamp was discarded. Then, pairs of the parameters and reference BPs acquired within an hour were averaged to minimize error in the reference BP measurement, as it was often measured in a bad posture or with motion artifacts, which may increase its unreliability. For example, if two pairs of the parameters and reference BPs were acquired at 14:00 and 14:30, respectively, they were averaged, which resulted in one pair of BP parameters and reference BPs for every hour. Because the daily pattern varied between subjects, and thereby the number of discarded data pairs owing to low quality of signal was different by subject, the number of collected datasets per subject was not the same.

G. DATA ANALYSIS

First, we assessed the changes in BP-related parameters (PAT, PTT, PEP, and SA) and BPs in each protocol. For the cycling protocol, five pairs of the parameters and BPs were averaged over the rest phase and exercise phase, regarded as baseline and perturbed values, and the group average difference between the two values was compared. For the HDU protocol, the early five pairs and late five pairs were considered as perturbed values and baseline values, respectively, and the group change was compared. In all these comparisons, the paired t-test was used with a significance level of $p < 0.05$.

Next, we calibrated the proposed model and other univariate models using PTT or PAT (listed in Table 1) to each reference BP for each subject. Then, we computed the mean

TABLE 1. Proposed model and other comparative models.

	Models for SBP		Models for DBP
1	$a \cdot PTT + b$	1	$a \cdot PTT + b$
2	$a \cdot PAT + b$	2	$a \cdot PAT + b$
3	$a \cdot \ln PTT + b$	3 *	$a \cdot \ln PTT + b$
4	$a \cdot \ln PAT + b$	4	$a \cdot \ln PAT + b$
5 *	$a \cdot \ln PTT + b \cdot SA + c$		

The models marked with an asterisk (*) are the models for SBP and DBP proposed in this study

absolute difference (MAD) between each calibrated BP and reference BP for all subjects. The MAD from the models was compared using the paired t-test. We used a significant level of p-value < 0.05. Similarly, SA was calibrated to the reference PP, and the MAD was computed.

To assess the generalization ability of the model, we derived optimal model coefficients from the subject group in the first study and applied them to the new subject group after simple calibration process. Then, the performance of the model was evaluated in accordance with the latest standard for wearable, cuffless blood pressure measuring devices published by the IEEE Engineering in Medicine and Biology Society, IEEE 1708-2014 [51].

The detailed process of deriving optimal model coefficients and calibration is as follows. Using all different combinations of coefficients from 0 to 100 for b and -100 to 0 for a in (9), we calculated the minimum mean squared error for each subject and summated the mean squared errors from all subjects. When we calculated the minimum mean squared error for each subject, constant c in (9) was considered a subject dependent variable as c will be replaced with a calibrated value in real practice. We selected the pair of coefficients that minimized the summated mean squared errors for all subjects as the optimal model coefficients. This work was repeated for the search of the optimal model coefficient a' for DBP in (10). In the calibration process, c and b' were adjusted for each extra subject in the second stage by calculating the individual initial differences between the reference and predicted BP (without calibration constants such as c and b') using initial BP measurements and parameters with the pre-determined optimal coefficients.

Using calibrated models for subjects, we calculated the MAD and correlation between the estimated and reference BP for all datasets from all subjects. Furthermore, the MAD was calculated for two groups of datasets within individual: the static and dynamic groups. The static group dataset consists of the three pairs of estimated and reference BPs after calibration and before the intervention for each subject, and the dynamic group dataset comprises the three pairs of estimated and reference BPs after the induced BP change.

To assess the BP estimation performance during a daily activity, the BP estimation model equipped with optimal coefficients derived in the second stage was applied to each subject with one-point measurement for calibration. Among the acquired datasets, the data point considered the most reliable and measured in the most stable condition was selected for calibration. Using the calibrated model, we estimated BPs and computed the MAD with reference BPs for each subject and the average of MAD values from all subjects was evaluated. Additionally, the estimated and reference BPs from all subjects were pooled and correlation coefficients between them were analyzed for SBP and DBP, respectively.

III. RESULTS

A. CHANGES IN PARAMETERS AND BPs IN DIFFERENT PROTOCOLS

Fig. 8 shows the changes in BP-related parameters and BPs with respect to the baseline in each protocol. In cycling, PP increased greatly compared to DBP (PP increased by 38.19±12.76% and DBP increased by 10.71±15.46%). The difference in BP between the baseline and perturbed values was significant. The BP-related parameters all changed in the opposite direction of BP. PTT and PEP decreased by 28.87±16.58% and 18.74±9.28%, respectively, and PAT, the sum of the two, decreased by 23.78±8.58%. SA showed a marked increase by 99.92±71.79%. The difference in the parameters between the baseline and perturbed values were significant. In the HDU protocol, SBP and DBP increased by 9.84±6.56% and 26.58±16.96%, respectively, whereas PP slightly decreased by −8.70±6.90%, which shows dominant changes in DBP compared to PP. The difference between the

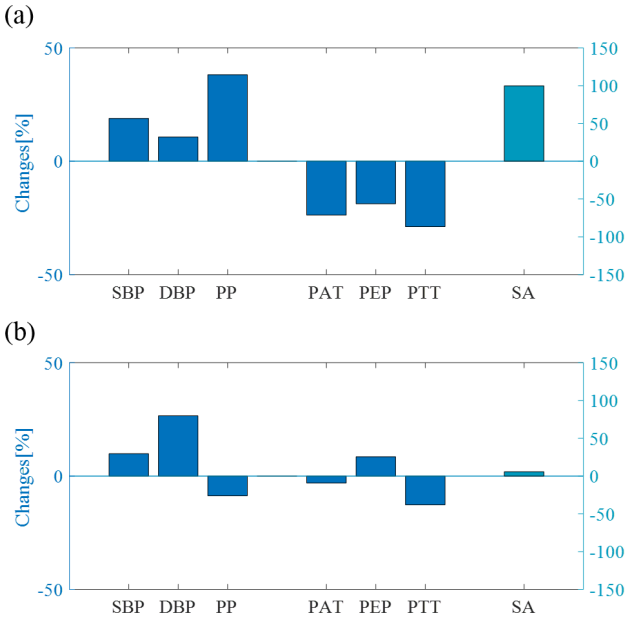

FIGURE 8. Changes in BP-related parameters and BPs. Changes in BP-related parameters and BPs with respect to (a) the rest phase in the cycling protocol and (b) beginning of the head-down to up change.

TABLE 2. Comparison of the parameters and BPS in two protocols.

	Cycling			Head down/up		
	BE	AE	Changes [%]	BR	AR	Changes [%]
SBP [mmHg]	118.12 ±11.56	139.88 ±9.26	18.91 ±7.19 *	106.94 ±14.24	116.95 ±12.05	9.84 ±6.56 *
DBP [mmHg]	78.62 ±15.07	85.64 ±12.02	10.71 ±15.46*	60.41 ±15.32	74.57 ±12.25	26.58 ±16.96 *
PP [mmHg]	39.49 ±7.44	54.24 ±9.78	38.19 ±12.76*	46.53 ±8.94	42.38 ±8.09	-8.70 ±6.90 *
PAT [ms]	150.39 ±17.93	115.37 ±23.59	-23.78 ±8.58 *	149.49 ±16.81	144.81 ±17.08	-3.07 ±5.07
PEP [ms]	81.15 ±13.30	65.00 ±5.89	-18.74 ±9.28 *	69.48 ±6.90	75.42 ±8.90	8.50 ±5.46 *
PTT [ms]	69.04 ±19.96	50.65 ±21.69	-28.87 ±16.58 *	80.01 ±14.02	69.39 ±10.32	-12.70 ±7.65 *
SA [au]	0.0080 ±0.0053	0.0160 ±0.0130	99.92 ±71.79*	0.0095 ±0.0070	0.0098 ±0.0069	5.76 ±18.76

The group averaged value of the parameters and BPs before exercise (BE) and after exercise (AE) was calculated, along with the changes in values in AE with respect to BE. The group averaged value of the parameters and BPs before reflex (BR) and after reflex (AR) was calculated, along with the changes in values in BR with respect to BE. The asterisk (*) indicates a significant difference between the two states ($p < 0.05$).

TABLE 3. Overall performance according to IEEE evaluation standard.

	SBP						DBP					
BP changes	MAD	MD	SD	CP5	CP10	CP15	MAD	MD	SD	CP5	CP10	CP15
Static test	4.05	0.18	5.54	68.33	96.67	98.33	2.50	0.16	3.63	90.00	98.33	98.33
BP change induced	9.73	6.43	9.00	18.33	50.00	83.33	4.81	-0.53	6.22	61.67	90.00	96.67
Total	6.89	3.31	8.07	43.33	73.33	90.83	3.66	-0.18	5.08	75.83	94.17	97.50

baseline and perturbed values was significant for all BPs. PTT decreased by 12.70±7.65%, as it did in the cycling protocol, while PEP increased by 8.50±5.46%, which was a different direction compared to that of the cycling protocol. PAT marginally decreased by 3.07±5.07%, and it showed the same direction as in the cycling protocol; however, the amount of change was very different in the two protocols. SA showed a slight increase by 5.76±18.76%. The difference between baseline and perturbed values was significant in PTT and PEP, but insignificant in PAT and SA. PTT changed the most consistently with BP in the two protocols. Table 3 presents the group mean and standard deviation of values of the BP-related parameters and BPs in the baseline and perturbed states for each protocol.

B. EFFICACY OF THE PROPOSED MODEL

The proposed model (model #5 for SBP and #3 for DBP) was calibrated to the reference BP to obtain subject-specific coefficients and the difference between the calibrated BPs and the reference BP was computed. Similarly, the performance of other models, including the widely used linear and logarithmic models using PTT or PAT as a sole parameter (model # 1–4), was compared. The performance between the linear model and logarithmic model was similar when using the same parameter (between model # 1 and 3 and model # 2 and 4). Thus, the proposed model for SBP (model #5) was compared to the logarithmic models (#3 and #4) for a more equivalent condition and model for DBP (model #3) was compared to the counterpart PAT model (model #4).

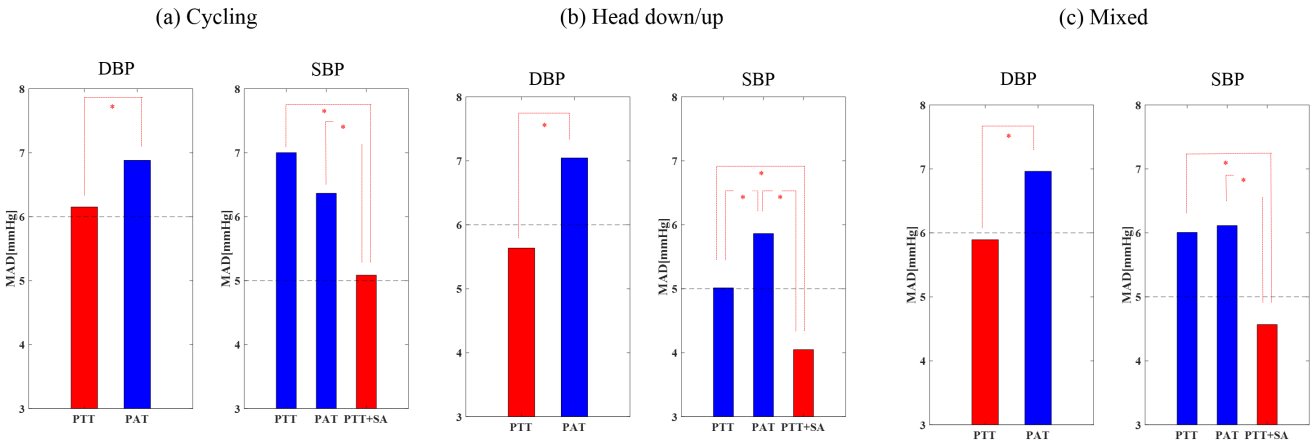

FIGURE 9. Performance comparison between models. On dataset from (a) the cycling and (b) HDU protocols, and (c) the two protocols combined (mixed) were compared. Asterisk (∗) indicates a significant difference ($p < 0.05$).

Fig. 9 shows the comparison between the proposed model and other models using PTT or PAT for the dataset from each protocol and for the dataset from the two protocols combined. Regarding the performance of the SBP estimation, a contrary performance of PTT and PAT in the two different types of intervention was clearly found. In the cycling protocol, the MAD when using PTT or PAT was of 7.00 and 6.37, respectively, showing better performance of PAT, although it was not a significant difference. On the contrary, the MAD of the proposed model was 5.09, showing a markedly better performance than that of the models using only PTT or PAT (27% and 20% of decrease with respect to the two counterparts, respectively). In the HDU protocol, the MAD when using PTT or PAT was of 5.01 and 5.86, respectively, which was a reversed result compared to that of the cycling protocol, showing better performance of PTT with a significant difference. Meanwhile, the MAD of the proposed model was 4.05, showing smaller errors than those of the models using only PTT or PAT (19% and 31% of decrease with respect to the two counterpart models, respectively). When two datasets from the two protocols were combined, the MAD of PTT and PAT was of 6.01 and 6.11, respectively, showing a similar level without significant difference, whereas the MAD of the proposed model was 4.57, showing a superior performance than that of the other two counterparts by a great margin (24% and 25% of decrease with respect to the two counterpart models, respectively).

In terms of the DBP estimation performance, the MAD of PTT for the cycling datasets, HDU datasets, and combined datasets from the two protocols, was of 6.15, 5.64, and 5.89, respectively, and that of PAT was of 6.88, 7.04, and 6.96, respectively. PTT showed consistently better results than PAT in all types of datasets.

Fig. 10(a), (b) show the correlation and Bland–Altman plots for the proposed model versus SBP and DBP. The proposed model, incorporating SA into the PTT model, yielded an excellent correlation ($r = 0.93$) with SBP.

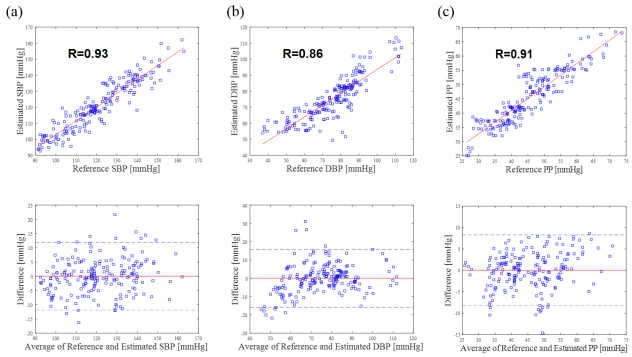

FIGURE 10. Correlation and Bland–Altman plots for estimated BPs versus reference (a) SBP, (b) DBP, and (c) PP.

The DBP estimation model, mostly adhering to a theoretical basis, also showed a tight correlation with the reference DBP ($r = 0.86$). The Bland–Altman plot verified that the variance of error was not biased, and most of the errors were within the limit of agreement, except for a few.

Fig. 10(c) shows the correlation and Bland–Altman plots for the calibrated PP using only SA versus the reference PP to assess the effect of SA as an indicator of PP. The correlation coefficient was 0.91, and most of the errors were also within the limit of agreement.

C. GENERALIZATION ABILITY

It was found that the optimal coefficients of a, b for SBP, and a' for DBP for the previous subject group were -20.04, 10.42, and -18.24, respectively. Table 3 presents the overall performance according to the IEEE standard when generalized to unseen new subjects. The overall MAD was of 6.89 for SBP and 3.66 for DBP, which is an acceptable level for the IEEE standard. As the IEEE standard recommends, the accuracy at different BP change levels is shown along with the accuracy at the static level, where the BP change

was not induced. The MAD at different BP change levels was greater than the overall accuracy, and the static level was lower than the overall one, as could be anticipated. Fig. 11 shows the distribution of the induced BP change as the IEEE standard requires. The induced SBP change was great, ranging up to 40 mmHg, and it was largely distributed between 15 to 35 mmHg. The ratio of number of data between 0–15 mmHg of BP changes and 15–30 mmHg of BP changes was approximately 56:44, similar to that of the IEEE standard, while the induced DBP change was narrow and mostly of less than 10 mmHg, which might cause the performance of the DBP estimation to appear relatively better than that of the SBP estimation.

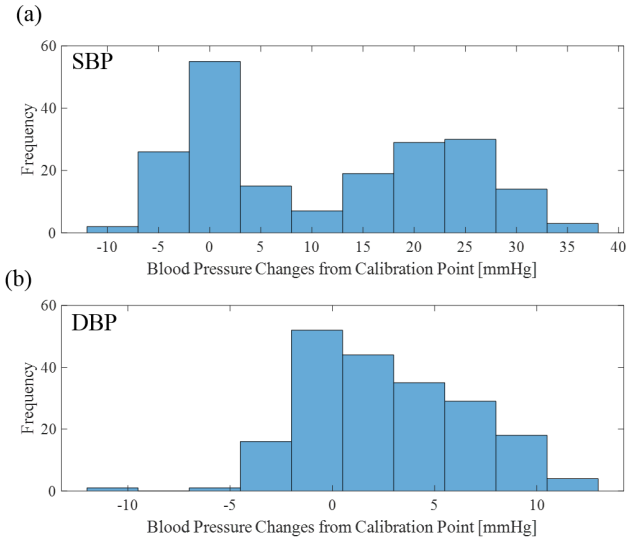

FIGURE 11. Distribution of induced BP change. (a) The induced SBP change was substantial, ranging up to 40 mmHg, and was largely distributed between 15 to 35 mmHg. (b) The induced DBP change was narrow and was mostly of less than 10 mmHg.

Fig. 12 shows the correlation and Bland–Altman plot between the estimated and reference BPs. The correlation coefficient between the estimated and reference SBP was

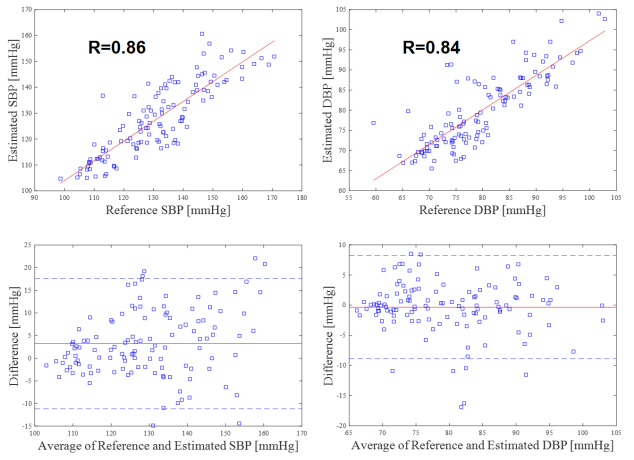

FIGURE 12. Correlation and Bland–Altman plot between estimated BPs with simple calibration and reference BPs.

0.86 and between the estimated and reference DBP was 0.84, which showed a tight correlation between the estimated and reference BPs, but lower than the correlation when using subject-specific coefficients. The correlation of SBP was slightly higher than that of DBP, although it may be attributed to the fact that the DBP change was smaller than the SBP distribution, which generally reduces the correlation coefficient and estimation error. The Bland–Altman plot indicates that the estimation errors were slightly positive-biased for SBP. As SBP increases, the errors tended to be more positive-biased, whereas as SBP decreases, the errors tended to be less biased. This tendency was not found in DBP, although a few errors were lower than the negative line of agreement. Overall, except for a few points, most of the errors were within the line of agreement.

D. DAILY MONITORING

Nine subjects participated in the daily monitoring stage. However, data from three subjects could not be used as less than half of the measurements were acquired, mainly owing to connection failure with the mobile application and signal degradation from excessive movements. More than 20 h of data were acquired from four subjects, and 17 h and 16 h of data were acquired from subjects 3 and 5, respectively.

Fig. 13 shows the typical trend of change in the reference (green boxes) and estimated (red line) BP by the proposed model during a day from subject 2. It should be noted that a nocturnal drop and a slight morning surge were captured by the proposed BP monitoring system.

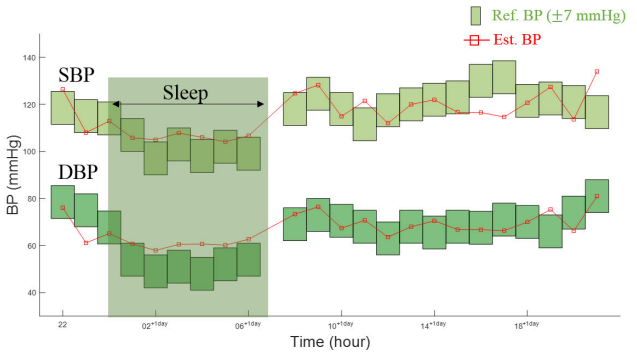

FIGURE 13. Typical example of trends in reference and estimated BP over 24 h in subject 2. The reference BP was indicated by green boxes with ± 7 mmHg of difference with the true value. The estimated BP by the proposed model is shown with the red line.

Fig. 14 shows the correlation and Bland–Altman plot for the estimated and reference BP. The correlation coefficients of SBP and DBP were 0.77 and 0.67, respectively. These values were much lower than the correlation coefficients from previous stages of the study, which may be attributed to various reasons, including the fact that the signal quality in daily life may be worse than that in controlled settings and the fact that the BP change was considerably limited in daily life, which lowers the correlation coefficient in general. The correlation coefficient of DBP was less than that of SBP, which may be explained by the fact that the personal variation

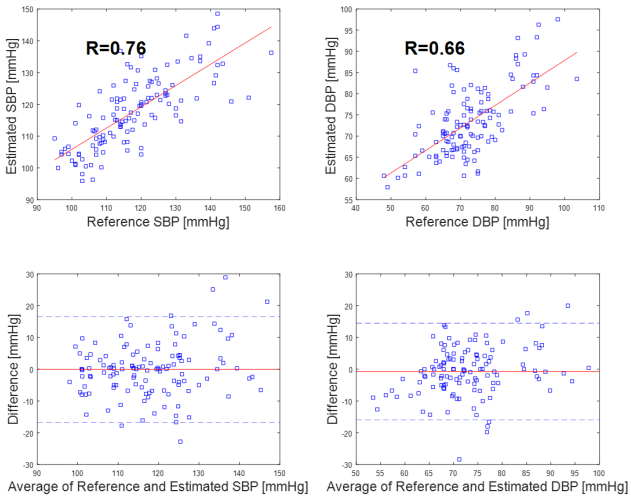

FIGURE 14. Correlation and Bland–Altman plot between estimated BPs and reference BPs in daily monitoring for six subjects.

of DBP was much less than that of SBP, which results in a narrow distribution of DBP in the pooled datasets.

Table 4 presents the individual and overall performance of BP estimation during daily monitoring. The MAD for SBP and DBP was of 5.87 and 5.63, respectively. During a day, approximately 30 mmHg of change was found in both SBP and DBP, which strengthens the necessity of daily BP monitoring.

TABLE 4. Individual and overall performance of BP estimation in daily monitoring.

Subject	SBP		DBP	
	MAD	Range	MAD	Range
1	9.41	112-157.5	8.44	57-103.5
2	6.08	97-131.5	5.26	48-84.5
3	3.77	105-131.5	4.90	66-81
4	4.33	97-124	5.70	57-85
5	6.74	113-151	4.36	57-76
6	5.94	95-120	5.58	58-82
Overall	6.04 ± 1.99	103.17-135.92	5.70 ± 1.42	57.17-85.33

IV. DISCUSSION

We sought to propose and validate a multivariate model, incorporating SCG amplitude (SA) into the conventional PTT–based model, with the newly developed wearable system. We compared the proposed and conventional models using PTT or PAT in two contrary interventions. Furthermore, we validated the proposed model with simple calibration process against unseen data from the separate subjects and demonstrated its real use in daily life. The results suggested that (1) the proposed model, which employed SA in conjunction with PTT for SBP estimation, outperformed the conventional univariate model using PTT or PAT (Fig. 9), and therefore, enabled independent estimation of SBP and DBP, which can often show different movements; (2) for practical use, the proposed model showed potential to be generalized (Table 3) after a simple calibration process, which is beyond the conventional subject-specific model fitting; and (3) the proposed model and system demonstrated the potential of continuous BP monitoring in daily life (Fig. 13) without any intervention of users or regulations.

A. PTT VS PAT

PAT has been used in many previous studies for its easy measurement. However, PAT is the sum of PTT and PEP, which is affected by various factors, including cardiac contractility, preload, and afterload [52], [53]. Thus, if PTT and PEP show conflicting movements in cases such as when there is an increase in afterload expressed by an increase in DBP, which accordingly shortens PTT and at the same time increases PEP [53], the change in PAT could be cancelled out by the different direction of change in PTT and PEP, and thereby it would not be well correlated with BP.

The developed wearable system was designed to provide PEP-excluded PTT by using the SCG AO point as proximal reference timing and PPG IT point as distal reference timing because PTT, the pure vascular transit time, is the one associated with BP based on the vessel wall property.

It was clearly found in this study that PEP showed different change with PTT (see Fig. 9) and the estimation performance of PAT was highly degraded accordingly (see Fig. 9(b)) when the afterload was perturbed, which is consistent with previous studies [13], [54] and the theory. However, it was also observed that PAT was very useful for SBP estimation (see Fig. 9(a)), significantly more than PTT in the cycling protocol, which was also often reported and has not been well understood in previous studies [17], [41], [42], [55]–[57]. One possible explanation is that PEP can better respond to hemodynamic changes than PTT in a dynamic exercise such as cycling [40]. As the dynamic exercise tends to increase SBP dominantly compared to DBP [44], the change in PTT can also be restricted. On the contrary, a decrease in PEP can be consistent owing to the increased cardiac contractility that instantly responds to activation of the sympathetic nerve during exercise in general [58], which accordingly results in a consistent decrease in PAT. The higher standard deviation of change in PTT than that of change in PEP and PAT in exercise (see Table 2) can support this explanation. Compared to SBP estimation, PTT showed better performance than PAT in DBP estimation regardless of type of intervention, which can support the importance of extracting PEP-excluded PTT for DBP estimation.

B. ENHANCEMENT OF PTT BASED BP ESTIMATION

Although it is obvious that one variable cannot explain two independent targets, as SBP and DBP show a tight correlation

in general, PTT has been serving as a common surrogate marker of both BPs in many previous studies. However, low correlation between SBP and DBP is often observed depending on the situation, which was pronounced when a subject cycled in this study. Cycling is one of the dynamic exercises where SBP generally increases, whereas DBP remains unchanged, compared to the static exercise, which increases both BPs [44]. During a dynamic exercise, the activated sympathetic nerve greatly increases HR and SV, and thus, CO, while TPR is generally decreased due to vascular dilation in the active muscle [44] in general. Depending on the subject and type of exercise, the proportion of increase in CO to decrease in TPR varies, which results in a relatively small increase in DBP or unchanged DBP, as DBP is closely affected by the combination of CO and TPR. On the contrary, the great increase in SBP is attributed to the increase in PP due to increased SV, which is mostly affected by cardiac ejection and arterial elastance. Thus, in the case when the change in SBP is dominant compared to that in DBP, the performance of BP estimation based on a change in PTT can be low owing to the fact that PTT is more associated with DBP, according to the theory, and that the change in PTT can be blurred by a measurement error when the change in DBP is narrow. It was clearly found in this study that SBP estimation based only on PTT is not satisfying, and even yields a worse result than PAT (See Fig. 9(a)). As the low correlation between BPs can be attributable to the effect of PP, whose change is not based on the conventional PTT–BP relationship, an independent indicator of PP may complement the BP estimation in particular cases.

Herein, we incorporated SA as an indicator of PP independent of PTT, thereby complementing the SBP estimation in conjunction with PTT. The combination of PTT and SA provided the improvement of the SBP estimation ($r = 0.93$) compared to those reported in the previous studies, such as 0.8 [13], 0.89 [59], 0.91 [60] for PTT with SBP, and 0.87 [55], 0.89 [9] for PAT with SBP, although the degree and intervention type of BP change were different. Using different combination of indicators for SBP and DBP will enable reliable and independent tracking of SBP and DBP. It was also found that SA was well correlated with PP in the two different interventions ($r = 0.78 \pm 0.13$; Fig. 8), and the correlation between the PP estimated by SA and reference PP was markedly high ($r = 0.91$, see Fig. 10(c)), which supports the potential of SA as an indicator of PP.

The relationship between SA and PP was inferred from the association of SA with cardiac ejection reported in previous studies [24], [25], [61]. This association may be explained by the fact that the first peak amplitude of SCG is mainly caused by the force of cardiac contraction [29], which is tightly associated with the amount of blood ejected to the aorta or, in other words, SV. The main factors of SV are the blood volume in LV in the end-diastole period, and cardiac contractility, which is the innate ability of the heart muscle to change in force. According to the length-tension relationship observed in the cardiac muscle, the increase in the blood volume in the LV in diastole stretches the cardiac muscle fibers, resulting in an increase in the force of cardiac contraction [62]. Besides, when cardiac contractility increases, the force of cardiac contraction obviously increases accordingly. Thus, increase in SV by either the blood volume in LV or cardiac contractility will accompany intensification in the force of cardiac contraction, which may increase peak amplitude of SCG.

C. GENERALIZATION ABILITY

The principle of PTT–BP relationship is subject-dependent as the equations describing the relationship between PTT and arterial elastance and between BP and arterial elastance depend on subject-specific parameters, such as the property of the blood vessel wall that varies by person. Thus, the majority of the presented works using the PTT–BP relationship have shown their performance using a subject-dependent calibration, which calibrated the model to the reference BP for each subject. However, this process generally requires BP changes, and measurements of BP and surrogate markers of BP during the BP changes, at least twice or more depending on the complexity of the model to derive the proportion of changes of the surrogate markers of BP to changes of BP for each subject, which is quite impractical and burdens a user. To alleviate the difficulty of the calibration process, we predetermined the coefficients of variates by using a modified least square method, which requires only one single measurement of BPs and the parameters within 1 min to apply it on a new subject. We derived the pre-determined model, tested the model for the datasets of different subject groups, and found that the group model could be applied to a new subject group, which was even larger than the subject group from which the model was derived, with a fairly small error range. It should be noted that the performance satisfied the IEEE standard, even though the pre-determined model was applied to new subjects with just an additional single measurement for individual calibration, which suggests that the proposed model using PTT and SA has the potential to be generalized with the simplified calibration process.

D. BP MONITORING IN DAILY LIFE

The current cuff-type devices providing ABPM are limited to their use by particular subjects, who already have been diagnosed in a clinic or pay attention to their BP status, owing to its highly discomforting aspect, especially during sleep. The results of the study by the proposed system design and model can provide ABPM more continuously than the conventional cuff-type ABPM, which is limited to use with intervals as short as approximately 15 min [43] without any requirement of a subject to intervene. Furthermore, as Fig. 13 demonstrates, this system can provide a way to assess the nocturnal drop without the discomfort of inflating and deflating a cuff, which could not be achieved by other recent studies of cuffless BP monitoring that require the subject to behave in a particular posture such as standing or sitting on a specialized apparatus [9], [17] and touching on a device with the fingertip [63]–[65]. Therefore, the proposed system could expand

the use of ABPM not only for subjects who are already on the risk of cardiovascular disease, but also for pre-hypertensive and normotensive subjects.

E. LIMITATIONS AND FUTURE WORK

This study has a few limitations that should be addressed in the future.

First, as the model validation was conducted among a limited population of young and healthy male subjects, the generalization ability of the model to various subject groups was not fully assessed. A future study should validate the proposed model against a more diverse population, including hypertensive and female subjects. It should be noted that, in the generalization, we derived the group model from subjects who are young and heathy, and applied it to those who can be regarded as homogeneous with the model-derived subject population. As the characteristic of the blood vessel wall could have homogeneity between subjects having similar vascular properties, the difference in the PTT–BP relationship can be prominent between normotensive and hypertensive subjects [66]–[68] and one's BP status could alter the PTT–BP relationship. Thus, this group model may not be applicable to a different population with subjects who are relatively older and hypertensive. However, as the young and normotensive subjects are those who lack compliance to daily BP monitoring and are mostly ignorant of their BP status, this convenient calibration process could increase the participation of this population into daily BP monitoring. This could allow early detection of their possible unwitting deterioration of the BP status, which otherwise could have not been detected. Second, the reference BP measurement may pose some limitations in the daily BP monitoring. Cuff-based BP measurement is influenced by the relative position of the arm with respect to the heart level. In other words, if the arm position is not aligned with the heart level, the measured BP is a sum of BP itself and hydrostatic pressure, depending on the height difference between arm and heart. In daily monitoring, especially during sleep, the arm position cannot be controlled, and thus, the relative position between arm and heart can be altered, which might result in an unreliable reference BP measurement. Moreover, when measuring the reference BP with an oscillometric BP measurement device, it is required that the subjects be in stable position when the reference BP is measured, which might prevent from observing the dynamic BP variation in daily life. Third, the relationship between SA and PP as well as the efficacy of the proposed model for SBP estimation is encouraged to be validated in BP changes from diverse circumstances such as mental pressure and cold pressor, as mechanisms of BP change from different circumstances may differ.

REFERENCES

[1] V. L. Burt, P. Whelton, E. J. Roccella, C. Brown, J. A. Cutler, M. Higgins, M. J. Horan, D. Labarthe, "Prevalence of hypertension in the US adult population: Results from the third national health and nutrition examination survey, 1988–1991," *Hypertension*, vol. 25, no. 3, pp. 305–313, 1995.

[2] P. K. Whelton, "Epidemiology of hypertension," *Lancet*, vol. 344, no. 8915, pp. 101–106, 1994.

[3] P. K. Whelton, T. V. Perneger, F. L. Brancati, and M. J. Klag, "Epidemiology and prevention of blood pressure-related renal disease," *J. Hypertension*, vol. 10, no. 7, pp. S77–S84, 1992.

[4] T. G. Pickering, N. H. Miller, G. Ogedegbe, L. R. Krakoff, N. T. Artinian, and D. Goff, "Call to action on use and reimbursement for home blood pressure monitoring: A joint scientific statement from the American heart association, american society of hypertension, and preventive cardiovascular nurses association," *Hypertension*, vol. 52, no. 1, pp. 10–29, 2008.

[5] F. S. Cattivelli and H. Garudadri, "Noninvasive cuffless estimation of blood pressure from pulse arrival time and heart rate with adaptive calibration," in *Proc. 6th Int. Workshop Wearable Implant. Body Sensor Netw. (BSN)*, 2009, pp. 114–119.

[6] W. Chen, T. Kobayashi, S. Ichikawa, Y. Takeuchi, and T. Togawa, "Continuous estimation of systolic blood pressure using the pulse arrival time and intermittent calibration," *Med. Biol. Eng. Comput.*, vol. 38, no. 5, pp. 569–574, 2000.

[7] L. Geddes, M. Voelz, S. James, and D. Reiner, "Pulse arrival time as a method of obtaining systolic and diastolic blood pressure indirectly," *Med. Biol. Eng. Comput.*, vol. 19, no. 5, pp. 671–672, 1981.

[8] J. Muehlsteff, X. Aubert, and G. Morren, "Continuous cuff-less blood pressure monitoring based on the pulse arrival time approach: The impact of posture," in *Proc. 30th Annu. Int. Conf. IEEE Eng. Med. Biol. Soc. (EMBS)*, Aug. 2008, pp. 1691–1694.

[9] Z. Tang, T. Tamura, M. Sekine, M. Huang, W. Chen, M. Yoshida, K. Sakatani, H. Kobayashi, and S. Kanaya, "A chair–based unobtrusive cuffless blood pressure monitoring system based on pulse arrival time," *IEEE J. Biomed. Health Inform.*, vol. 21, no. 5, pp. 1194–1205, Sep. 2017.

[10] X. Ding, B. P. Yan, Y.-T. Zhang, J. Liu, N. Zhao, and H. K. Tsang, "Pulse transit time based continuous cuffless blood pressure estimation: A new extension and a comprehensive evaluation," *Sci. Rep.*, vol. 7, no. 1, p. 11554, 2017.

[11] R. Mukkamala, J.-O. Hahn, O. T. Inan, L. K. Mestha, C.-S. Kim, H. Töreyin, and S. Kyal, "Toward ubiquitous blood pressure monitoring via pulse transit time: Theory and practice," *IEEE Trans. Biomed. Eng.*, vol. 62, no. 8, pp. 1879–1901, Aug. 2015.

[12] G. Zhang, M. Gao, D. Xu, N. B. Olivier, and R. Mukkamala, "Pulse arrival time is not an adequate surrogate for pulse transit time as a marker of blood pressure," *J. Appl. Physiol.*, vol. 111, no. 6, pp. 1681–1686, 2011.

[13] S. L.-O. Martin, A. M. Carek, C.-S. Kim, H. Ashouri, O. T. Inan, J.-O. Hahn, and R. Mukkamala, "Weighing scale-based pulse transit time is a superior marker of blood pressure than conventional pulse arrival time," *Sci. Rep.*, vol. 6, p. 39273, Dec. 2016.

[14] J. Y. A. Foo and C. S. Lim, "Dual-channel photoplethysmography to monitor local changes in vascular stiffness," *J. Clin. Monitor. Comput.*, vol. 20, no. 3, pp. 221–227, 2006.

[15] R. A. Payne, C. N. Symeonides, D. J. Webb, and S. R. J. Maxwell, "Pulse transit time measured from the ECG: An unreliable marker of beat-to-beat blood pressure," *J. Appl. Physiol.*, vol. 100, no. 1, pp. 136–141, 2006.

[16] J. Solá, M. Proença, D. Ferrario, J.-A. Porchet, A. Falhi, O. Grossenbacher, Y. Allemann, S. F. Rimoldi, and C. Sartori, "Noninvasive and nonocclusive blood pressure estimation via a chest sensor," *IEEE Trans. Biomed. Eng.*, vol. 60, no. 12, pp. 3505–3513, Dec. 2013.

[17] C. S. Kim, A. M. Carek, R. Mukkamala, O. T. Inan, and J. O. Hahn, "Ballistocardiogram as proximal timing reference for pulse transit time measurement: Potential for cuffless blood pressure monitoring," *IEEE Trans. Biomed. Eng.*, vol. 62, no. 11, pp. 2657–2664, Nov. 2015.

[18] J. Nürnberger, S. Dammer, A. O. Saez, T. Philipp, and R. Schäfers, "Diastolic blood pressure is an important determinant of augmentation index and pulse wave velocity in young, healthy males," *J. Hum. Hypertension*, vol. 17, no. 3, p. 153, 2003.

[19] W. B. Kannel, T. Gordon, and M. J. Schwartz, "Systolic versus diastolic blood pressure and risk of coronary heart disease: The Framingham study," *Amer. J. Cardiol.*, vol. 27, no. 4, pp. 335–346, 1971.

[20] B. Gavish, I. Z. Ben-Dov, and M. Bursztyn, "Linear relationship between systolic and diastolic blood pressure monitored over 24 H: Assessment and correlates," *J. Hypertension*, vol. 26, no. 2, pp. 199–209, 2008.

[21] J. Blacher, J. A. Staessen, X. Girerd, J. Gasowski, L. Thijs, L. Liu, J. G. Wang, R. H. Fagard, and M. E. Safar, "Pulse pressure not mean pressure determines cardiovascular risk in older hypertensive patients," *Arch. Internal Med.*, vol. 160, no. 8, pp. 1085–1089, 2000.

[22] A. M. Dart and B. A. Kingwell, "Pulse pressure—A review of mechanisms and clinical relevance," *J. Amer. College Cardiol.*, vol. 37, no. 4, pp. 975–984, 2001.
[23] M. D. Rienzo, E. Vaini, P. Castiglioni, G. Merati, P. Meriggi, G. Parati, A. Faini, and F. Rizzo, "Wearable seismocardiography: Towards a beat-by-beat assessment of cardiac mechanics in ambulant subjects," *Autonomic Neurosci.*, vol. 178, nos. 1–2, pp. 50–59, 2013.
[24] K. Tavakolian, "Characterization and analysis of seismocardiogram for estimation of hemodynamic parameters," Ph.D. dissertation, Dept. Appl. Sci., Simon Fraser Univ., Burnaby, BC, Canada, 2010.
[25] K. Tavakolian, A. P. Blaber, B. Ngai, and B. Kaminska, "Estimation of hemodynamic parameters from seismocardiogram," in *Proc. Comput. Cardiol.*, 2010, pp. 1055–1058.
[26] J. M. Zanetti and K. Tavakolian, "Seismocardiography: Past, present and future," in *Proc. 35th Annu. Int. Conf. IEEE Eng. Med. Biol. Soc. (EMBC)*, Jul. 2013, pp. 7004–7007.
[27] V. Gemignani, E. Bianchini, F. Faita, M. Giannoni, E. Pasanisi, E. Picano, and T. Bombardini, "Operator-independent force-frequency relation monitoring during stress with a new transcutaneous cardiac force sensor," in *Proc. Comput. Cardiol.*, 2007, pp. 737–740.
[28] T. Bombardini, V. Gemignani, E. Bianchini, L. Venneri, C. Petersen, E. Pasanisi, L. Pratali, M. Pianelli, F. Faita, M. Giannoni, and E. Picano, "Cardiac reflections and natural vibrations: Force-frequency relation recording system in the stress echo lab," *Cardiovascular Ultrasound*, vol. 5, no. 1, p. 42, 2007.
[29] I. Korzeniowska-Kubacka, M. Bilińska, and R. Piotrowicz, "Usefulness of seismocardiography for the diagnosis of ischemia in patients with coronary artery disease," *Ann. Noninvasive Electrocardiol.*, vol. 10, no. 3, pp. 281–287, 2005.
[30] R. Crow, P. Hannan, D. Jacobs, L. Hedquist, and D. M. Salerno, "Relationship between seismocardiogram and echocardiogram for events in the cardiac cycle," *Amer. J. Noninvasive Cardiol.*, vol. 8, no. 1, pp. 39–46, 1994.
[31] N. Gaddum, J. Alastruey, P. Beerbaum, P. Chowienczyk, and T. Schaeffter, "A technical assessment of pulse wave velocity algorithms applied to non-invasive arterial waveforms," *Ann. Biomed. Eng.*, vol. 41, no. 12, pp. 2617–2629, 2013.
[32] D. Korteweg, "Ueber die Fortpflanzungsgeschwindigkeit des Schalles in elastischen Röhren," *Annalen der Physik*, vol. 241, no. 12, pp. 525–542, 1878.
[33] A. Moens, "Over de voortplantingssnelheid van den pols [On the speed of propagation of the pulse]," Tech. Rep., Leiden, The Netherlands, 1877.
[34] A. Moens, "Die pulskurve [the pulse curve]," Leiden, The Netherlands, Tech. Rep., 1878.
[35] W. Milnor, *Hemodynamics*. Baltimore, MD, USA: Williams & Wilkins, 1982.
[36] D. Hughes, C. F. Babbs, L. Geddes, and J. Bourland, "Measurements of Young's modulus of elasticity of the canine aorta with ultrasound," *Ultrason. Imag.*, vol. 1, no. 4, pp. 356–367, 1979.
[37] J. Sola, S. F. Rimoldi, and Y. Allemann, "Ambulatory monitoring of the cardiovascular system: The role of pulse wave velocity," in *New Developments in Biomedical Engineering*. Rijeka, Croatia: InTech, 2010.
[38] A. Steptoe, H. Smulyan, and B. Gribbin, "Pulse wave velocity and blood pressure change: Calibration and applications," *Psychophysiology*, vol. 13, no. 5, pp. 488–493, 1976.
[39] B. Gribbin, A. Steptoe, and P. Sleight, "Pulse wave velocity as a measure of blood pressure change," *Psychophysiology*, vol. 13, no. 1, pp. 86–90, 1976.
[40] J. Muehlsteff, X. Aubert, and M. Schuett, "Cuffless estimation of systolic blood pressure for short effort bicycle tests: The prominent role of the pre-ejection period," in *Proc. 28th Annu. Int. Conf. IEEE Eng. Med. Biol. Soc. (EMBS)*, 2006, pp. 5088–5092.
[41] H. Gesche, D. Grosskurth, G. Küchler, and A. Patzak, "Continuous blood pressure measurement by using the pulse transit time: Comparison to a cuff-based method," *Eur. J. Appl. Physiol.*, vol. 112, no. 1, pp. 309–315, 2012.
[42] M. Masé, W. Mattei, R. Cucino, L. Faes, and G. Nollo, "Feasibility of cuff-free measurement of systolic and diastolic arterial blood pressure," *J. Electrocardiol.*, vol. 44, no. 2, pp. 201–207, 2011.
[43] G. Lopez, M. Shuzo, H. Ushida, K. Hidaka, S. Yanagimoto, Y. Imai, A. Kosaka, J.-J. Delaunay, and I. Yamada, "Continuous blood pressure monitoring in daily life," *J. Adv. Mech. Design, Syst., Manuf.*, vol. 4, no. 1, pp. 179–186, 2010.
[44] G. R. Bezucha, M. Lenser, P. Hanson, and F. Nagle, "Comparison of hemodynamic responses to static and dynamic exercise," *J. Appl. Physiol.*, vol. 53, no. 6, pp. 1589–1593, 1982.
[45] K. Patel, A. Rössler, H. K. Lackner, I. Trozic, C. Laing, D. Lorr, D. A. Green, H. Hinghofer-Szalkay, and N. Goswami, "Effect of postural changes on cardiovascular parameters across gender," *Medicine*, vol. 95, no. 28, p. e4149, 2016.
[46] C. McCrory, L. F. Berkman, H. Nolan, and N. O'leary, M. Foley, and R. A. Kenny, "Speed of heart rate recovery in response to orthostatic challenge," *Circulat. Res.*, vol. 119, no. 5, pp. 666–675, 2016.
[47] S. S. Zambrano and D. H. Spodick, "Comparative responses to orthostatic stress in normal and abnormal subjects: Evaluation by impedance cardiography," *Chest*, vol. 65, no. 4, pp. 394–396, 1974.
[48] V. Cooper and R. Hainsworth, "Effects of head-up tilting on baroreceptor control in subjects with different tolerances to orthostatic stress," *Clin. Sci.*, vol. 103, no. 3, pp. 221–226, 2002.
[49] S. Reulecke, S. Charleston-Villalobos, A. Voss, R. González-Camarena, J. González-Hermosillo, M. J. Gaitán-González, G. Hernández-Pacheco, R. Schroeder, and T. Aljama-Corrales, "Orthostatic stress causes immediately increased blood pressure variability in women with vasovagal syncope," *Comput. Methods Programs Biomed.*, vol. 127, pp. 185–196, Apr. 2016.
[50] J. Suzuki, T. Nakamura, M. Hirayama, Y. Mizutani, A. Okada, M. Ito, H. Watanabe, and G. Sobue, "Impaired peripheral vasoconstrictor response to orthostatic stress in patients with multiple system atrophy," *Parkinsonism Rel. Disorders*, vol. 21, no. 8, pp. 917–922, 2015.
[51] *IEEE Standard for Wearable Cuffless Blood Pressure Measuring Devices*, IEEE Standard 1708-2014, 2014.
[52] O. T. Inan, D. Park, L. Giovangrandi, and G. T. A. Kovacs, "Noninvasive measurement of physiological signals on a modified home bathroom scale," *IEEE Trans. Biomed. Eng.*, vol. 59, no. 8, pp. 2137–2143, Aug. 2012.
[53] J. Krohová, B. Czippelová, Z. Turianiková, Z. Lazarová, I. Tonhajzerová, and M. Javorka, "Preejection period as a sympathetic activity index: A role of confounding factors," to be published.
[54] M. Gao, N. B. Olivier, and R. Mukkamala, "Comparison of noninvasive pulse transit time estimates as markers of blood pressure using invasive pulse transit time measurements as a reference," *Physiological Rep.*, vol. 4, no. 10, p. e12768, 2016.
[55] M. Y.-M. Wong, C. C.-Y. Poon, and Y.-T. Zhang, "An evaluation of the cuffless blood pressure estimation based on pulse transit time technique: A half year study on normotensive subjects," *Cardiovascular Eng.*, vol. 9, no. 1, pp. 32–38, 2009.
[56] C. Ahlstrom, A. Johansson, F. Uhlin, T. Länne, and P. Ask, "Noninvasive investigation of blood pressure changes using the pulse wave transit time: A novel approach in the monitoring of hemodialysis patients," *J. Artif. Organs*, vol. 8, no. 3, pp. 192–197, 2005.
[57] Y. Yoon, J. H. Cho, and G. Yoon, "Non-constrained blood pressure monitoring using ECG and PPG for personal healthcare," *J. Med. Syst.*, vol. 33, no. 4, pp. 261–266, Aug. 2009.
[58] K. T. Larkin and A. L. Kasprowicz, "Validation of a simple method of assessing cardiac preejection period: A potential index of sympathetic nervous system activity," *Perceptual Motor Skills*, vol. 63, no. 1, pp. 295–302, 1986.
[59] A. Esmaili, M. Kachuee, and M. Shabany, "Nonlinear cuffless blood pressure estimation of healthy subjects using pulse transit time and arrival time," *IEEE Trans. Instrum. Meas.*, vol. 66, no. 12, pp. 3299–3308, Dec. 2017.
[60] X.-R. Ding, Y.-T. Zhang, J. Liu, W.-X. Dai, and H. K. Tsang, "Continuous cuffless blood pressure estimation using pulse transit time and photoplethysmogram intensity ratio," *IEEE Trans. Biomed. Eng.*, vol. 63, no. 5, pp. 964–972, May 2016.
[61] P. Castiglioni, A. Faini, G. Parati, and M. Di Rienzo, "Wearable seismocardiography," in *Proc. 29th Annu. Int. Conf. IEEE Eng. Med. Biol. Soc. (EMBS)*, Aug. 2007, pp. 3954–3957.
[62] R. Klabunde, *Cardiovascular Physiology Concepts*. Philadelphia, PA, USA: Lippincott Williams & Wilkins, 2011.
[63] N. Watanabe, Y. K. Bando, T. Kawachi, H. Yamakita, K. Futatsuyama, Y. Honda, H. Yasui, K. Nishimura, T. Kamihara, T. Okumura, H. Ishii, T. Kondo, H. Ishii, T. Kondo, and T. Murohara, "Development and validation of a novel cuff-less blood pressure monitoring device," *Basic Transl. Sci.*, vol. 2, no. 6, pp. 631–642, 2017.

[64] A. Chandrasekhar, C.-S. Kim, M. Naji, K. Natarajan, J.-O. Hahn, and R. Mukkamala, "Smartphone-based blood pressure monitoring via the oscillometric finger-pressing method," *Sci. Transl. Med.*, vol. 10, no. 431, p. eaap8674, 2018.
[65] K. Matsumura, P. Rolfe, S. Toda, and T. Yamakoshi, "Cuffless blood pressure estimation using only a smartphone," *Sci. Rep.*, vol. 8, no. 1, p. 7298, 2018.
[66] N. R. Gaddum, L. Keehn, A. Guilcher, A. Gomez, S. Brett, P. Beerbaum, T. Schaeffter, and P. Chowienczyk, "Altered dependence of aortic pulse wave velocity on transmural pressure in hypertension revealing structural change in the aortic wall," *Hypertension*, vol. 65, no. 2, pp. 362–369, 2015.
[67] K. Ng, M. Butlin, and A. P. Avolio, "Persistent effect of early, brief angiotensin-converting enzyme inhibition on segmental pressure dependency of aortic stiffness in spontaneously hypertensive rats," *J. Hypertension*, vol. 30, no. 9, pp. 1782–1790, 2012.
[68] M. Butlin, F. Shirbani, E. Barin, I. Tan, B. Spronck, and A. Avolio, "Cuffless estimation of blood pressure: Importance of variability in blood pressure dependence of arterial stiffness across individuals and measurement sites," *IEEE Trans. Biomed. Eng.*, vol. 65, no. 11, pp. 2377–2383, Nov. 2018.

JONGHYUN PARK received the B.S. degree in electrical and computer engineering and the M.S. and Ph.D. degrees in biomedical engineering from Seoul National University, Seoul, South Korea, in 2013, 2015, and 2019, respectively.

From 2013 to 2019, he performed researches on biomedical system development and physiological modeling at the Medical Electronics Laboratory (MELab), Seoul National University. His research interests include developing non-invasive cardiovascular physiological monitoring systems and biomedical signal processing.

SEUNGMAN YANG received the B.S. degree in electrical and computer engineering from Seoul National University, Seoul, South Korea, in 2016, where he is currently pursuing the Ph.D. degree in bioengineering.

His research interests include developing non-invasive cardiovascular physiological monitoring systems and biomedical signal processing.

JANGJAY SOHN received the B.S. degree in biomedical engineering from Yonsei University, Wonju, South Korea, in 2016, and the M.S. degree in biomedical engineering from Seoul National University, Seoul, South Korea, in 2018, where he is currently pursuing the Ph.D. degree in biomedical engineering. His research interests include developing wearable cardiovascular devices and biomedical signal processing.

JOONNYONG LEE was born in Seoul, South Korea, in 1989. He received the B.S. and M.Eng. degrees in biomedical engineering from Boston University, in 2014, and the Ph.D. degree in bioengineering from Seoul National University, in 2019.

From 2014 to 2019, he was a Research Assistant with the Medical Electronics Laboratory, Seoul National University. Since 2019, he has been a Research Professor with the Biomedical Research Institute, Seoul National University Hospital. He has published articles in biomedical engineering and biosignal processing and has patented multiple inventions. His research interests include machine learning, biosignal processing, and physiological modeling.

SARAM LEE received the Ph.D. degree in the interdisciplinary program for biomedical engineering from Seoul National University, in 2014. He studied physiological monitoring system and biomedical signal processing under supervision of Prof. H. C. Kim. Since 2014, he has been a Research Professor with the Biomedical Research Institute, Seoul National University Hospital. His current research interests include ubiquitous healthcare devices, biosensors, and its valuation.

YUNSEO KU (M'18) received the B.S. degree in electrical engineering and the M.S. and Ph.D. degrees in biomedical engineering from Seoul National University, Seoul, South Korea, in 2004, 2008, and 2017, respectively. From 2008 to 2018, he performed researches on biomedical circuits and systems for mobile healthcare applications at the Samsung Advanced Institute of Technology, Suwon, South Korea. He is currently an Assistant Professor with the Department of Biomedical Engineering, College of Medicine, Chungnam National University, Daejeon, South Korea. His research interests include biomedical system design and neuromodulation technologies for neurological disorders.

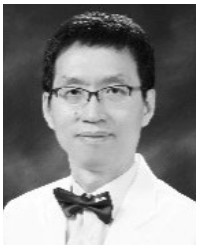

HEE CHAN KIM (M'95) received the Ph.D. degree in control and instrumentation engineering (biomedical engineering major) from Seoul National University, Seoul, South Korea, in 1989. From 1989 to 1991, he was a Staff Engineer working on the National Institute of Health (NIH)-funded electrohydraulic total artificial heart project at the Artificial Heart Research Laboratory, The University of Utah, Salt Lake City, UT, USA. He joined the Faculty of the Department of Biomedical Engineering, College of Medicine, Seoul National University, and the Seoul National University Hospital, in 1991, where he is currently a Professor leading the Medical Electronics Laboratory (MELab). Major research activities in the MELab include the development of intelligent algorithms and electronic instrumentations for medical and biological applications, including artificial organs (such as artificial heart and artificial pancreas), biosensors, ubiquitous/mobile healthcare systems, and man–machine interface. In these areas, he has published over 180 peer-reviewed scientific articles in international journals and holds more than 170 patents. He is also a member of the Korea Society of Medical and Biological Engineering (KOSOMBE), the IEEE/EMBS, and the American Society of Artificial Internal Organs (ASAIO).